PERGAMON

Engineering Fracture Mechanics 63 (1999) 57–80

Engineering Fracture Mechanics

Application of coupled brittle–ductile model to study correlation between Charpy energy and fracture toughness values

L.C.A. Folch, F.M. Burdekin*

Department of Civil and Structural Engineering, UMIST, PO Box 88, Manchester, M60 1QD, UK

Received 15 September 1997; received in revised form 2 November 1998; accepted 18 December 1998

Abstract

A coupled brittle–ductile fracture local approach model has been developed to predict either Charpy energy or fracture toughness and to investigate conditions for correlations between them. A modification to the Beremin model has been introduced to assess failure in individual elements and make it compatible with the Lemaitre model for implementation as a user subroutine for the program ABAQUS. A probabilistic based fracture criterion was introduced to monitor the damage within individual elements by either cleavage or ductile tearing. The fracture toughness and Charpy energy for a nuclear industry steel BPL A508 were determined for the transition temperature range using finite element analyses with three-dimensional solid elements for both the standard 25 mm SE(B) three-point bend specimen and the Charpy 45° V-notch specimen. Prescribed failure probabilities of 0.05, 0.5 and 0.95 were imposed as critical values to predict the scatter of fracture toughness experimental data. The evaluation of constraint, equivalent plastic strain and maximum principal stress amongst other parameters gave the basis for comparison of the response of the two geometries. Critical values of fracture stress in the modified Beremin model for cleavage fracture and of the Lemaitre damage parameter for ductile fracture were calibrated from experimental fracture toughness data. These same critical values were then used in the analysis of the Charpy specimens, including allowance for strain rate effects, and good agreement found between predicted and experimental energy absorption values. The only conditions where the maximum constraint and equivalent plastic strain in the two specimen geometries were found to match were at the temperature for 28 J energy absorption in the Charpy impact energy and that for fracture toughness, K_{IC}, of 100 MPa-m$^{1/2}$ for the BPL A508 steel. This may be an important factor in the correlation between Charpy and fracture toughness tests proposed by Wallin.

* Corresponding author. Tel.: +44-161-200-4600; fax: +44-161-200-4601.

0013-7944/99/$ - see front matter
PII: S0013-7944(99)00009-0

1. Introduction

The Charpy impact test was introduced in the late 1940 s as a standard material test for welded steel construction, as a result of studies carried out on ships which suffered unstable brittle fractures. In a number of cases unstable fracture occurred over a great portion of the cross section of the ship at mid-length when local critical load and residual stress conditions were reached in service at cold ambient temperatures [1,2]. The results of catastrophic failure of such structures by unstable crack propagation raised the safety question of structures for a wide range of applications. It was not until the 1960 s, however, that Charpy test requirements were introduced into British Standards for bridges, buildings, low temperature pressure vessels and storage tanks. The Charpy impact test is a commercial quality control test for steels and other alloys used in the construction of metallic structures. The test allows the material properties for service conditions to be determined experimentally in a simple manner with a very low cost. Charpy impact tests on steels over a range of temperatures show clearly a change in the failure mode accompanied by a sudden change in the energy absorbed from brittle cleavage fracture and a lower shelf energy at low temperatures to ductile tearing fracture and an upper shelf energy at higher temperatures. The transition temperature is defined as the temperature range over which the change in energy values from the lower to the upper shelf takes place.

The steels used in the nuclear industry, like many others, have to be selected to prevent brittle fracture by means of specified fracture toughness properties. This specified value for fracture toughness is usually based on the stress intensity factor parameter, K_{IC}. The material fracture toughness, measured as the plane-strain lower-bound toughness, K_{IC}, can be determined in specimens containing a single-edge deep crack subjected to slow bend loading, either directly as a critical stress intensity factor if failure occurs within the linear elastic regime, or by means of the J-integral (or CTOD) if yielding occurs before fracture. The J-integral (or CTOD) produces a more suited measurement of material toughness, particularly in the transition and upper-shelf regimes, where the effects of crack tip plasticity may be significant. Thus the evaluation of the fracture toughness can be carried out by converting elastic–plastic J-integral values to K_{IC} values, which is common practice for structural design and engineering applications based on failure assessment diagram methods.

The correlation between the Charpy energy and the fracture toughness in terms of K_{IC}, has been the object of study by several authors e.g. [3–5], and consequently a number of empirical formulations relating values of Charpy impact energy to fracture toughness have been produced. A recent compilation of these is given by Phaal et al. [6]. The importance of establishing a correlation between a quality control measure for material fracture toughness, such as the Charpy energy, and a value more suited for design, such as the critical stress intensity factor K_{IC}, can be justified by the need of designers for producing safer structures and accurate engineering predictions. The Charpy impact test related to material fracture toughness plays an important part in many material specifications in which its values are used to establish design minimum requirements for steels and metal alloys at minimum service temperatures in order to meet satisfactory safety levels. In particular the empirical formulation proposed by Wallin [5] based on the development of an early correlation put forward by Marandet and

Sanz [4] has proved to be effective in predicting fracture toughness values, K_{IC}, from the knowledge of the temperature at which the Charpy energy is equal to 27 J. This formulation has been studied in the present work by looking into the internal local approach parameters that might explain and justify the Wallin correlation.

Continuum damage mechanics models have been developed, mainly for ductile fracture of yielding materials. These micromechanical models take account of constraint effects and material imperfections to calculate the actual strain and stress fields around cracks or defects in materials. The local approach method consists of application of continuum damage mechanics using a very fine finite element mesh to predict fracture. Also brittle fracture has been modelled by statistical approach models based on probability of unstable fracture due to cleavage. The use of Weibull statistics for modelling of defect distributions over a characteristic volume of material under a critical state of stress allows the probability of general unstable fracture to be predicted. The local approach uses internal microscale variables related to the material damage evolution in order to predict the initiation of macroscale cracks in an elastic–plastic regime. This methodology has been an invaluable complement for classical fracture mechanics which is based on a single parameter for characterising fracture but does not reproduce the transitional behaviour satisfactorily.

An attempt has been made in the present work to characterise the correlation between fracture toughness and Charpy energy using a coupled brittle–ductile damage (CBDD) model. The model was calibrated to predict the mean values and scatter of the static fracture toughness of the BPL A508 steel based on elastic–plastic FE and J-integral calculations for a standard single-edge cracked three-point bend specimen over the material transition temperature range. The Charpy impact energy was determined using the model with the local approach parameters from the calibration of the fracture toughness specimen geometry over the transition range temperature for the same steel, BPL A508. The bi-modal fracture behaviour of the material in the Charpy test was investigated in the present model by taking

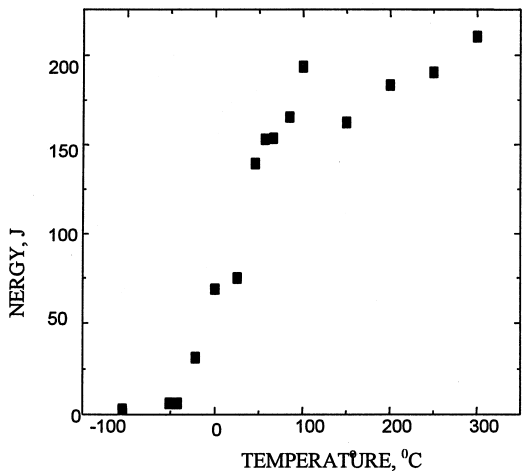

Fig. 1. Experimental Charpy impact energy data for BPL A508 Class 3 from AEA reference [7].

into account material strain rate-dependency effects also. The model is intended to reproduce the whole fracture process from fracture initiation to the final fracture through a sequence of partial crack extensions. Three-dimensional finite element analyses were carried out throughout the present work to study the constraint effects on transition behaviour more effectively.

2. Material

Experimental results of Charpy impact energy and material fracture toughness tests were available from an AEA report [7] for a BPL A508 Class 3 steel in the quenched and tempered condition over a range of temperatures between 80°C down to −150°C and these are plotted in Figs. 1 and 2, respectively. The yield strength, ultimate tensile strength, elastic modulus, strain hardening exponent and Poisson's ratio were also available for the same range of temperatures. The A508 forging is a typical nuclear industry steel, produced by Creusot–Loire in the mid 1970 s, used for construction of the thick wall forged rings of pressurized water reactors. The chemical composition of the forging is summarized in Table 1. The heat treatment of the material carried out by AEA Technology was an initial treatment of 1 h at 1050°C with a furnace cool, followed by an austenization process holding for 10 h at 880°C after heating at a rate of 30°C/h. The quench rate was 6°C/min and the final tempering treatment was held 20 h at 675°C with a heating rate of 30°C/h.

The material fracture toughness tests carried out by AEA Technology consisted of slow bend tests of standard single-edge-notched (SENB) bend specimens and 25 mm thick plane-sided compact tension (CT) specimens, fatigue pre-cracked in accordance with ASTM E813 standard to obtain a length/width ratio (a/W) of approximately 0.55. The specimens were tested at a ram displacement rate of 0.5 mm/min at one of a number of temperatures in the range −150–80°C, covering the lower shelf and the full transition region. Specimens were loaded until either

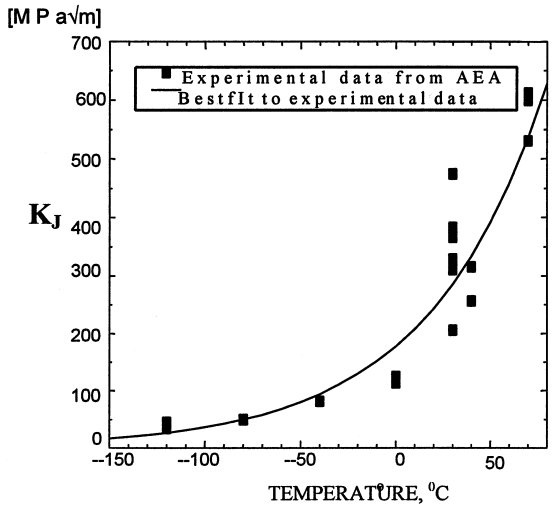

Fig. 2. Experimental fracture toughness data for BPL A508 Class 3 from AEA reference [7].

Table 1
Chemical composition of the BPL A508 Class 3 forging

C	Si	Mn	P	S	Cu	Ni	Cr	Mo	Al	As	Sb	Sn	V	Ti
Percentage of weight										ppm				
0.153	0.23	1.33	0.008	0.008	0.05	0.70	0.15	0.50	0.027	240	20	48	18	38

they fractured by cleavage, or the applied stress intensity factor (K) derived from the J-integral, reached about 700 MPa $m^{1/2}$. The crack growth resistance curve showing amount of ductile tearing corresponding to the toughness results in Fig. 2 at temperatures of 30°C and above is shown in Fig. 3. Tension tests were carried out to determine the uniaxial tensile mechanical properties for the material under slow rate loading for the range of temperatures above.

3. Local approach coupled brittle–ductile fracture model

A coupled brittle–ductile damage (CBDD) fracture model has been developed for implementation as a user subroutine in the standard finite element program ABAQUS [8]. The model considers both fracture mechanisms brittle cleavage and ductile tearing in local approach applications in the transition temperature range by implementing modifications of the Beremin [9] and Lemaitre [10] models. These models have been coupled to predict fracture initiation and propagation by either of the mechanisms wherever the respective critical values for the local fracture criterion are reached first. A fully probabilistic approach has been

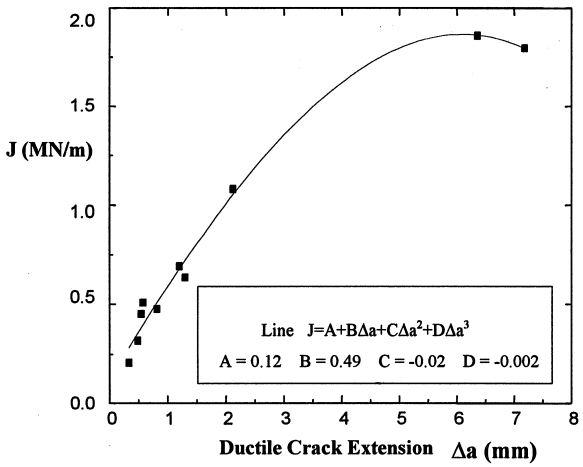

Fig. 3. R curve data for A508 steel [7].

implemented in the CBDD model taking advantage of the probabilistic nature of the modified Beremin model and using structural reliability concepts to calculate the probability of ductile failure based on the damage variable in Lemaitre's model. Tolerances for the calculated probability of failure due to either brittle or ductile fracture have been imposed as the failure criteria. The standard Beremin model is based on the weakest link theory which considers the total failure of the structure as the sum of the individual probabilities of failure of each element in a system in series. The coupled brittle–ductile model developed by Folch [11], however, is based on a system of elements connected in parallel in which the probability of failure of the individual elements is calculated independently and the global failure of the specimen or structure occurs when all the component elements have failed. This makes the brittle and ductile failure models compatible and the parameters in both models are computed simultaneously as a function of the solution variables in the finite element program.

Failure of the element or structural component involves the progressive diminution of the carrying capacity of the material at a particular load and location. This is achieved by decreasing the stiffness matrix in the elements where failure criteria have been reached, i.e. reducing the value of the modulus of elasticity. The two separate fracture criteria are monitored for any particular point at each load increment to check whether the critical values have been exceeded for either of the failure mechanisms. Due to the different nature of the fracture mechanisms, the post fracture material behaviour is controlled, for each of the fracture mechanisms, by an independent factor applied to the rate of diminution of the material stiffness. In other work the local approach parameters have been found to be sensitive to the degree of finite element mesh refinement in fracture mechanics applications, but one advantage of the present work is that both fracture mechanisms are dealt with using the same mesh.

The standard Beremin model [9] calculates the probability of failure, due to unstable cleavage, based on the hypothesis of finding a microcrack of a critical size in an element of a characteristic volume under a stress state, σ. The defects in the material follow the Weibull distribution and the nominal Weibull stress is a function of the volume of material considered and the distribution of the maximum principal stress. The Beremin model considers that microcracks should be open due to local plastic strain in order to produce unstable fracture. Thus the Weibull stress is calculated over the plastic region and consequently the probability of failure is determined for the geometry being analysed. The parameters in the Beremin model are the critical cleavage stress, σ_u, a characteristic volume of material related to the grain size, V_o, and the shape parameter for the Weibull probability distribution, m.

The modified Beremin model considered in the present work is based on the same principles of Weibull statistics for the distribution of the defects and their size as the standard Beremin model [9]. The probability of finding a microcrack of a critical size between l_0 and $l_0 + \mathrm{d}l_0$ under a stress state σ within a volume of material V_0 is given below [9]:

$$P(l_0)\mathrm{d}l_0 = \frac{\alpha}{l_0^{\beta}}\mathrm{d}l_0 \tag{1}$$

where α and β are material constants for a given characteristic volume for the material, V_0, which must include a certain number of grains within which it is expected that a defect of a critical size will occur. If σ is the maximum principal stress which causes a microcrack to open,

then the probability of brittle fracture of an individual volume V_0 is given by the expression:

$$P(\sigma) = \left(\frac{\sigma}{\sigma_u}\right)^m \tag{2}$$

where $m = 2(\beta - 1)$. If all the elements of a component are considered to be connected in parallel, the probability of failure for the whole component depends on the failure of each and every one of the constituent elements. The difference between this approach and the standard Beremin model [9] is basically that the probability of fracture of the entire specimen is calculated using weakest link theory rather than a continuum mechanics algorithm to assess probability of failure of individual elements. The Weibull statistical parameters must be adjusted from the modified Beremin model to match experimental data in order to produce reliable results. In particular, the σ_u parameter is considered to produce the failure of just one smaller element in the modified model instead of an assembly of elements forming the whole specimen as in the standard model.

In the present coupled brittle–ductile model the Weibull stress was computed for every individual element undergoing plastic strain, independently, and the model parameters were scaled to the size of finite element mesh. This requires, however, that the stress within the element of volume V^j should be almost constant such that the statistical requirements for the validity of the Beremin formulation are met.

The Lemaitre [10] model is based on thermodynamics principles to define the plastic strain potential for continuum mechanics. An internal damage variable is related to the dissipative strain energy which measures the overall damage evolution, as the total area of microvoids in a section of a finite volume of material. The damage variable is independent of shape and size of the defects, but is a function of the direction of the normal to the plane which contains the defects. The concept of effective stress is introduced to evaluate the stress as the force per effective unit area of material. The constitutive relations for the evolution of damage in the material are expressed as a function of the triaxial state of stress and the total plastic strain, and this model assumes that the mechanical effects of cavities and microcracks are the same in compression and tension. The hypothesis of strain equivalence assumes that the effect of damage on the strain behaviour is modified through the effective stress.

The modified Gurson model [12], which incorporates a yield function for porous metal plasticity, was also utilized in the present work in conjunction with the Lemaitre and Beremin models. This yield condition function is available as a mechanical constitutive model for plasticity in the later versions of ABAQUS standard, and is given by the following expression [8]:

$$\Theta = \left(\frac{q}{\sigma_y}\right)^2 + 2q_1 f \cosh\left(-\frac{3}{2}\frac{q_2 p}{\sigma_y}\right) - (1 + q_3 f^2) = 0 \tag{3}$$

where q is the von Mises stress, p is the hydrostatic pressure, f is the volume fraction of the voids in the material and σ_y is the yield strength. If $f = 0$, Eq. (3) for the Gurson yield condition reduces to the von Mises expression. The coefficients q_1, q_2 and q_3 are those introduced by Tvergaard to the Gurson model. The Lemaitre model does not depend on the

yield condition function and so this model was used to determine the ductile fracture condition in conjunction with the modified Gurson model to determine yielding conditions.

In the CBDD model the ductile damage variable was calculated for each element as a function of the solution variables in the finite element analysis of both fracture toughness and Charpy specimens. The probability of failure was obtained from the reliability index which was evaluated from typical distributions of the damage variable determined during the previous FE analyses within the calibration process for each particular temperature and specimen geometry. The mean value and standard deviation of the damage variable were chosen assuming a normal distribution. Thus at each increment of load in the FE analysis for calculation of the fracture toughness or Charpy energy and for each integration point, the instantaneous value of the damage variable and the critical value D_c allowed the probability of ductile fracture to be calculated.

The introduction of the probabilistic approach to the ductile damage calculation enables both failure mechanism criteria to be included in the coupled model as probabilistic treatments in a fully compatible manner.

4. Application to study correlation between CVN and K_{IC}

Most of the correlations between fracture toughness and Charpy impact energy formulations are restricted to the specific material for which they have been validated based on experimental data. Some of these correlations are more general and can be applied to more than one material, for instance for low and medium strength steels. A few of the existing formulations seem able to make predictions for general applications such as low, medium and high strength steels and aluminium alloys. One of the few correlations between fracture toughness and Charpy impact energy which produces good predictions for general applications, is Wallin's formulation [5]. In the present work this particular correlation has been studied in order to compare predictions using the CBDD model and Wallin's correlation.

The correlations are based on a single fracture mechanics parameter, K_{IC} or J_{IC}, related to Charpy energy and very little is known about the reason for this correlation. In applications such as those required for the nuclear industry, a more detailed fracture assessment for the material is necessary and over the last few years proposals have been made to introduce a second parameter to take account of constraint effects on fracture toughness [13–17]. Constraint is the effect which inhibits yielding due to a triaxial stress system, thus allowing the maximum principal stress to reach higher levels. It can be quantified by the ratio of hydrostatic to equivalent stress, but recent work has shown that this is closely related to T and Q stress ratios which are non-singular second-order linear and non-linear terms, respectively, in the expression for stress fields around the crack tip expanded in series. These parameters have been calculated by some authors [13,14,16] at a certain characteristic location from the crack tip region which yields a measure of constraint. It is to be expected that constraint will also be sensitive to strain rate at the root of the notch in the Charpy specimen and at the crack front in the standard fracture toughness specimen in view of the concentration of plastic strain and this will be discussed in Section 4.2. This makes it difficult to apply constraint-based T and Q approaches in their present form directly to the Charpy specimen. The local approach offers an

alternative method for characterization of the stress and strain fields around highly stressed areas based on internal variables representative of damage evolution in the material, which takes into account constraint effects and material imperfection.

In the present study the fracture toughness and the Charpy energy absorption of the BPL A508 steel were determined over a range of temperatures using the CBDD model in order to assess the correlation between both quantities. The application of the coupled local approach model in the transition temperature range required that the brittle model and ductile model parameters were properly tuned to match the experimental data available from Ref. [7]. The finite element analyses used eight-node three-dimensional solid elements and the input data for material properties were the uniaxial tensile test results. The internal parameters in the CBDD model were kept the same for both geometries throughout the analyses once they had been tuned.

The parameters in both the modified Beremin and Lemaitre models were tuned by using the results of the non-linear finite element analyses of the fracture toughness bend specimen at different temperatures in the range -100 to 70°C. The probability of fracture by both brittle and ductile mechanisms was calculated at each load increment and the corresponding J value was determined from the work done under the load–load point displacement curve in the FE analyses. At the J value which corresponded to the fracture toughness from the experimental data, the critical values of σ_u and m for the modified Beremin model and D_c for the Lemaitre model were recorded for each particular temperature. These values were then used in the determination of the Charpy energy without modification, with the exception of the solution dependent variable which controls the change in material properties in the program after failure takes place which was adjusted to give the best match to the Charpy experimental data. The failure mechanism for initiation of crack growth in the bend specimen was determined automatically in the models as a function of the stress and strain fields around the crack front area. Brittle failure required high values of stress with low plastic strain whilst ductile failure generally required significant amounts of plastic strain to occur. The elements at the crack front itself were monitored for crack growth initiation by either failure mechanism, whichever occurred first. For the temperatures concerned no overlap of mechanism took place. The number of elements involved in the initiation of the crack growth process was determined by the failure mechanism itself, with brittle fracture at low temperatures tending to be unstable involving a larger number of elements across the specimen thickness. On the other hand, the onset of pure ductile tearing started at midthickness and did not extend immediately to the edge but spread progressively across the thickness as load increments were applied. For temperatures in the transition range fracture initiation tended to be brittle at mid thickness with a tongue in the ligament direction.

4.1. Material fracture toughness calculation

Finite element analyses of the standard three-point bend specimen were carried out for the BPL A508 Class 3 steel for determination of K_{IC}. The geometry analysed in this work was the standard 25 mm three-point bend test published by the American Society for Testing Materials, ASTM E813 [23] with initial crack depth ratio a/W of 0.5 and span to width ratio S/W of 4. Static analyses were carried out using three-dimensional (3D) solid elements with

eight nodes for the three-point bend specimen geometry. Taking advantage of the double symmetry of the specimen, a quarter of the geometry was modelled with the mesh shown in Fig. 4, imposing the necessary boundary conditions to simulate the whole geometry behaviour. The elements immediately ahead of the crack tip in the ligament direction were $0.625 \times 0.5 \times 0.694$ mm. Analyses of sensitivity were carried out for the effects of refining mesh size and the mesh shown in Fig. 4 was the finest mesh possible taking account of limitations of available computer CPU time and memory limitations. To check on this, a comparison of the results of FEA analysis for the ratio of maximum principal stress to yield strength was carried out for a two-dimensional (2D) analysis using elements of area 50×50 μm and for the 3D mesh in Fig. 4 at a temperature of 70°C. These results are given in Fig. 5 and show the stress distribution ahead of the crack tip at two different load line displacements Δ, for both conditions, namely 2D plane strain and an actual three-dimensional state of stress. The differences in the geometry response for different element type and mesh size conditions are due to the third component of stress along the thickness in the 3D analysis which affects the maximum principal stress in a way not present in the 2D analysis.

The results show that the mesh size for the 3D analysis gives a sufficiently accurate description of the maximum principal stress when compared to the finer mesh of the 2D analysis. The use of a finer 3D mesh would not give a much better stress distribution or results closer to the 2D plane strain results. The differences between the 2D and 3D results are due to the fact that the stress in the thickness direction is constant for the 2D case whilst the 3D elements show that this is not true for extensive plasticity regions where constraint is high.

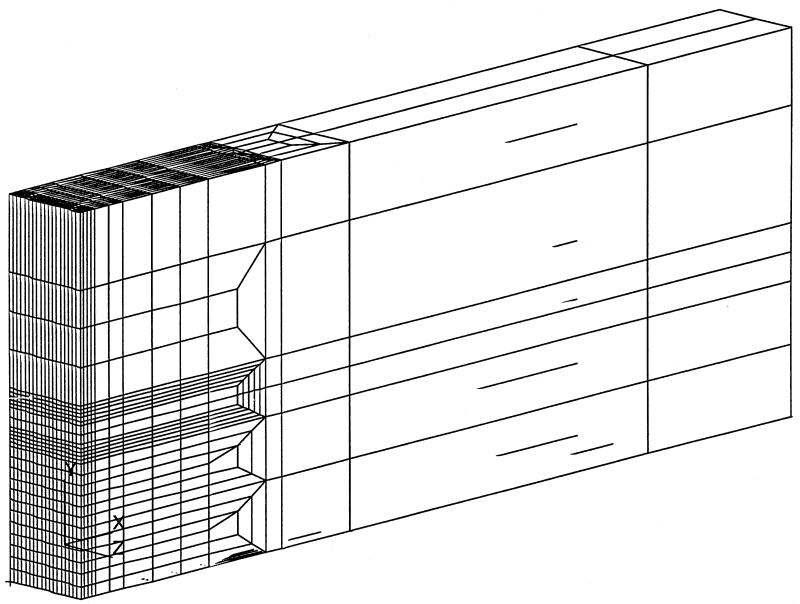

Fig. 4. Finite element mesh for the standard SE(B) three-point bend specimen.

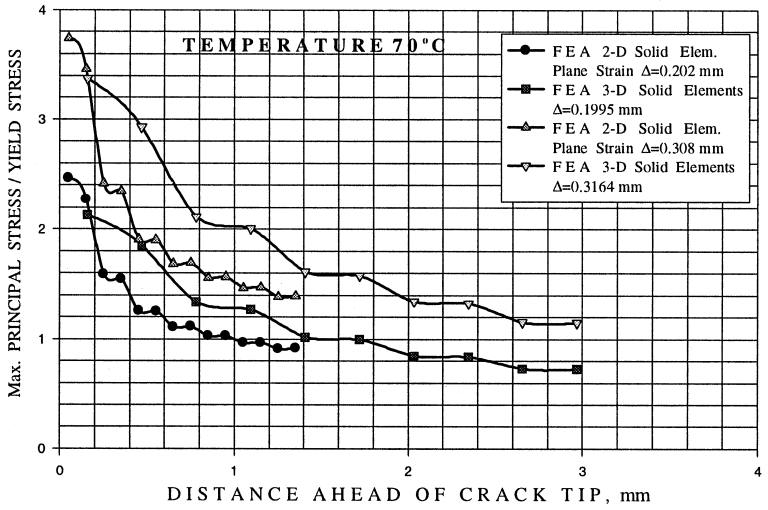

Fig. 5. FEA results for maximum principal stress/yield stress ratio for the mesh size sensitivity study for 2D elements and 3D solid elements in the standard three-point bend specimen (SE(B)).

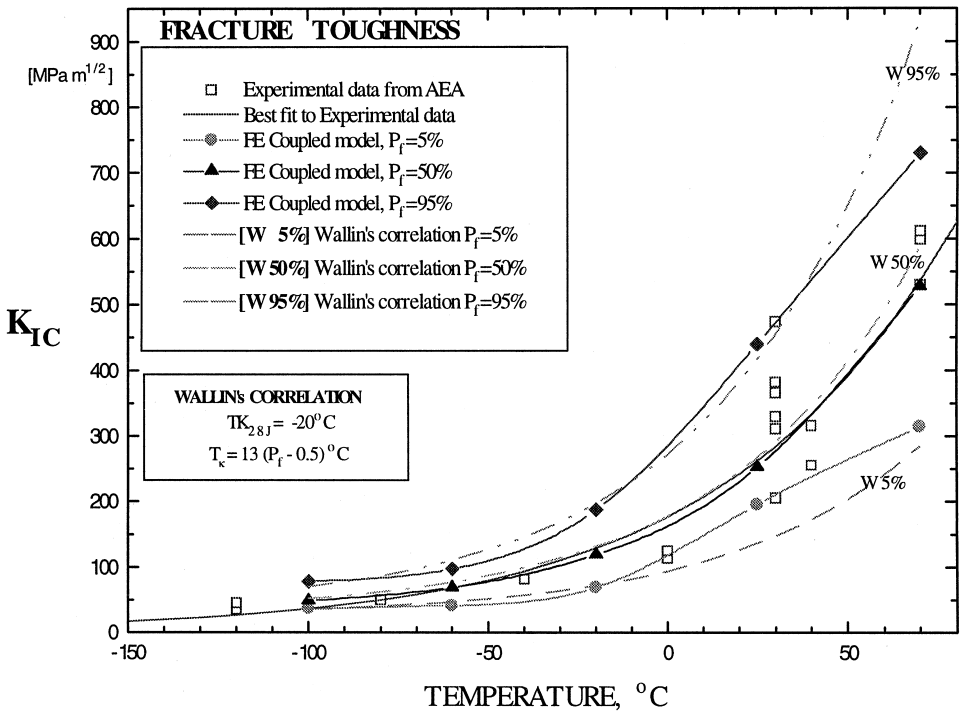

Fig. 6. Comparison of Wallin's formulation fracture toughness estimates with experimental data from AEA reference [7] and FEA results using the coupled damage model for the BPL A508.

Furthermore the mesh size in Fig. 4 produced satisfactory predictions of fracture toughness based on the FEA and probability calculations using the modified Beremin model.

The specific materials data used as input for the FE analyses were the uniaxial true stress-strain curve, the work hardening exponent, the elastic modulus and Poisson's ratio for the various temperatures analysed from Ref. [7].

The use of the CBDD Model allows the initiation of crack growth to be estimated from the fracture criteria implemented in the ABAQUS subroutine. The local fracture criteria were the probability of brittle/ductile fracture as discussed previously.

The critical values for fracture initiation were tuned to match the experimental results as described above, with the following details.

The fracture toughness data presented in Fig. 2 were fitted to curves of the form:

$$\ln K_J = \ln A + BT \tag{4}$$

as shown in Fig. 6, where the values of A and B chosen to give the best fit to the data were $A = 177$ MPa$\sqrt{\text{m}}$ with standard error 3, and $B = 0.0158/^{\circ}\text{C}$ with standard error 0.001. In Eq. (4) T is the temperature in °C and K_J is the transition fracture toughness corresponding to the ductile–brittle transition temperature (DBTT) estimated by Ortner et al. as 250 MPa$\sqrt{\text{m}}$ [7].

The outcomes of CBDD analysis were the critical cleavage stress σ_u and the shape parameter m for the Weibull statistics of the modified brittle fracture model as shown in Table 2, together with the critical values of the Lemaitre damage variable D_c for all the temperatures considered. It would be equally possible to use data from notched tensile tests at each temperature to carry out the calibration, but this data was not available in the present case.

Results of stress ratios and constraint values calculated for the standard bend specimen and for the Charpy specimen (see later) at initiation of crack growth are included in Figs. 7–9 as a function of temperature. The critical values of stress ratios corresponding to the conditions at initiation in the standard bend specimen were compared to stress ratios at the notch or crack front for the Charpy specimen for three different conditions: (i) at initiation of crack growth, (ii) the maximum value registered during the whole fracture process and (iii) the mean value obtained during the fracture process. Critical values of the stress ratios for a crack extension of 1 mm as well as at the instability point, which correspond to the crack arrest for upper shelf temperatures, and final fracture for lower shelf temperatures are also included in Figs. 8 and 9. Figs. 7–9 show the pattern and magnitude of the critical values of stress ratios in the local approach models for both specimen geometries.

The results of the application of the local approach CBDD model to the calculation of the fracture toughness for the BPL A508 Class 3 steel over the range of temperatures −100°C to 70°C are plotted in Fig. 6, where the experimental data from Ref. [7] are also included.

Three FE analyses were carried out for each temperature with the probability of brittle–

Table 2
Variation of critical, σ_u and parameter m with temperature for the BPL A508 Class 3 steel

T(°C)	−100	−60	−20	25	70
m	15	15	15	21	21
σ_u (MPa)	1340	1628	1875	2140	2200

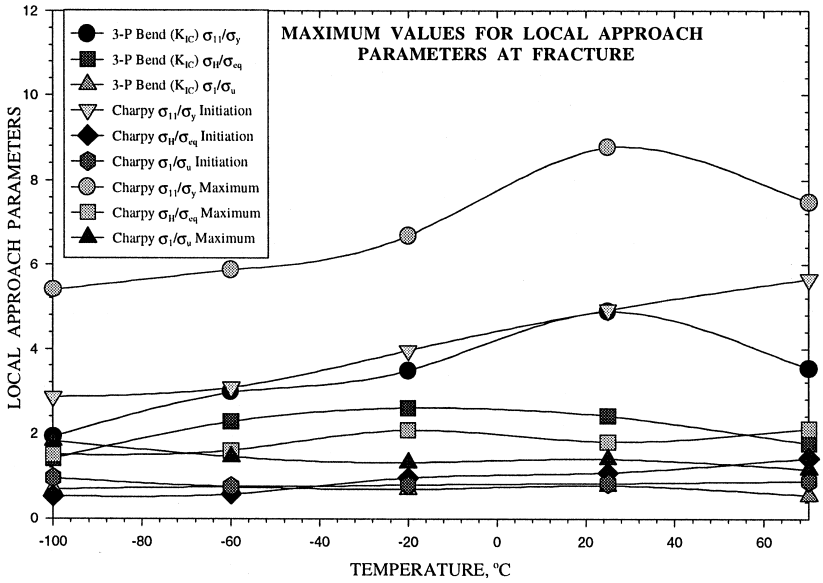

Fig. 7. Comparison of the maximum values of the local approach parameters for the three-point bend specimen and Charpy specimen for the BPL A508 Class 3 steel.

ductile fracture set at 5%, 50% and 95% in order to evaluate the scatter in the results. Values of J were found from the work done under the load versus load line displacement curve from the FE analysis for the specimen and converted to equivalent K_{IC} values by the relationship:

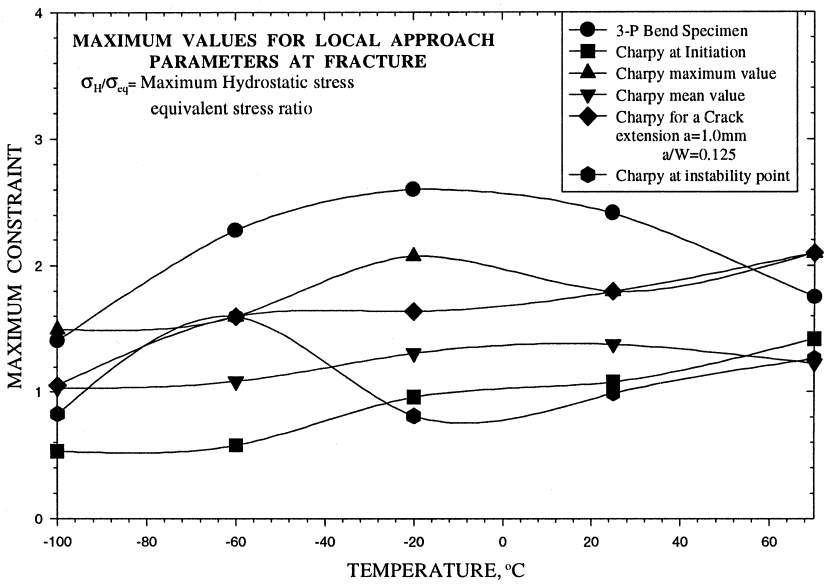

Fig. 8. Comparison of the maximum values of the constraint for the three-point bend specimen and the Charpy specimen for the BPL A508.

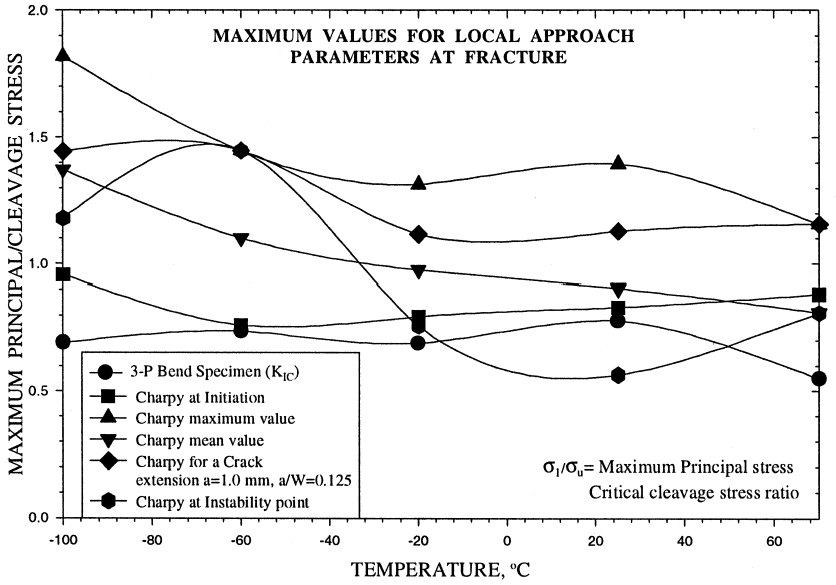

Fig. 9. Comparison of the maximum values of the max principal stress/cleavage stress ratio for the three-point bend specimen and the Charpy specimen for the BPL A508.

$$K_{IC} = \sqrt{\frac{EJ_{IC}}{(1-\upsilon^2)}} \tag{5}$$

In Fig. 6, all the values of fracture toughness over 300 MPa$\sqrt{m}$, determined either experimentally or numerically, correspond to ductile crack growth initiation. The calibration of the critical parameters in the coupled model, as discussed above, allowed the predictions of brittle and ductile fracture to be adjusted in such a way that the scatter of the experimental data is limited at the upper bound by the FEA results at the $P_f = 0.95$ curve and at the lower bound by the $P_f = 0.05$ curve. The curve for the FEA results at $P_f = 0.5$ coincides with the main curve for the experimental data. Thus a reliable tuning of the parameters of the coupled model was achieved and these values were then used in the predictions of Charpy impact energy.

4.2. Charpy impact energy determination

The Charpy test consists of applying an impact load by a pendulum striker to the test piece supported at each end to produce total or partial fracture, such that the energy absorbed in the fracture process can be determined by subtracting the final potential energy from the initial potential energy of the striker. The striker speed at the moment of impact should be between 5 and 5.5 m/s. The Charpy test standard specimen geometry consists of a bar 55 mm long and 10×10 mm square cross section with a single V-notch, 2 mm deep and 0.25 mm root radius, in

one face at mid-length and a span between supports of 40 mm. The standard notch flank angle is 45°. The finite element mesh for one quarter of the specimen geometry is shown in Fig. 10.

Finite element analyses were carried out for the Charpy specimen geometry using eight-node 3D solid elements with the CBDD model subroutine for ABAQUS. Material strain rate-dependent uniaxial tensile properties were used to simulate the dynamic mechanical behaviour of the material under impact loading. The effect of the notch in the Charpy specimen geometry produces an increase of the effective strain rate below the root of the notch due to a concentration of plastic strain which raises the yield strength by strain hardening and also a local triaxial stress state. The dynamic effects of the impact load produce an increase in the yield strength, for the uniaxial tensile properties, as a direct consequence of the fast rate of straining.

Experimental work on dynamic tensile tests [18,19] and plastic deformation of cantilever beams subject to impulsive load [20] have shown an increase in the uniaxial yield strength as a function of the strain rate. Gerard also showed the increase of the yield strength for a biaxial stress–strain dynamic test and the uniaxial stress–strain curve for strain rate-dependent material can be modelled by the strain-rate power law:

$$\dot{\varepsilon} = D\left(\frac{\sigma_y}{\sigma_o} - 1\right) \tag{6}$$

where σ_y is the dynamic yield strength, σ_o is the static yield strength and D and p material characteristics. The values of D and p in Eq. (6) were set to 40.4 and 0.2, respectively. These values were recommended by Bodner and Symond [20] for mild steels and the same values have been assumed in many other applications for steels other than mild steels. Data for the particular A508 steel was not available but this was bypassed because of the low sensitivity to

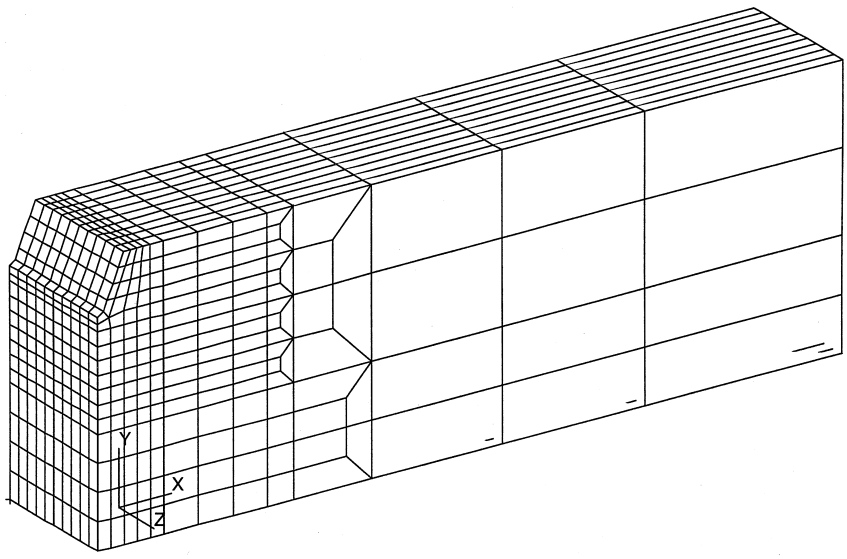

Fig. 10. Finite element mesh for the Charpy specimen geometry.

D and p for the strain rate relevant to the Charpy specimen of the order of 400 s^{-1}. With values of D between 20 and 400, combined with values of p of 0.2 or 0.1, the variation in the ratio dynamic/static yield strength lies in the range 2.0 to 2.8 and at the assumed values the ratio was 2.59.

The use of the local approach to model the Charpy specimen geometry solves the problem of increased local strain by using a refined mesh at the root of the notch and by introducing strain rate-dependent material properties. Thus the notch geometry effects are properly covered with the fine mesh shown in Fig. 10 in which the elements underneath the root of the notch are $0.5\times0.5\times0.25$ mm and the next elements are $0.5\times0.5\times0.5$ mm. The uniaxial tensile material mechanical properties were corrected for the strain rate at the root of the notch. The strain rate for initiation of fracture was determined from a preliminary finite element analysis using the static stress-strain curve as a function of the speed of the striker at the moment of impact by the expression

$$\dot{\varepsilon} = \frac{\Delta\varepsilon}{\Delta u}\,\frac{\mathrm{d}u}{\mathrm{d}t} \tag{7}$$

where $\Delta\varepsilon$ is the strain increment at the root of the notch for an increment of the load line displacement, Δu, and $\mathrm{d}u/\mathrm{d}t$ is the striker speed at the moment of impact. No attempt was made to model the change in strain rate or any effects of adiabatic heating as the crack advanced although to some extent these effects would tend to oppose each other. The increase in the uniaxial yield stress was obtained as a function of the strain rate by substituting (7) in expression (6). As noted above, the ratio dynamic/static yield stress was 2.59 obtained from the strain magnitude at the moment of impact. The work hardening exponent was changed between dynamic and static mechanical properties, by keeping the plastic portion of the stress–strain curve the same for dynamic and static cases but displacing it vertically to match the relevant yield strength. The elastic modulus was not altered for the dynamic stress–strain curve used as the input data for the uniaxial tensile properties in the coupled brittle–ductile damage model.

The inertia effects produced by the acceleration of the specimen reported in instrumented impact tests are eliminated by the quasi-static finite element analysis as the specimen is being "monitored" instead of the striker. Oscillation problems are overcome by modelling the specimen supports as rolling supports, constraining the load line direction displacement by applying the correct boundary conditions. The effect of dilatational stress waves was considered as negligible based on the specimen size and the time for the waves to travel the specimen width. Using the elastic properties for the BPL A508 steel the time, t_W, for a wave to travel the width of the specimen for the Charpy geometry was calculated as 1.97×10^{-5} s for an unbounded dilatational wave speed, c_1, 5.075×10^5 mm/s. The transition time, t_T, introduced by Nakamura [21] as the time beyond which dynamics effects are decreasing in the specimen due to the absorption of the striker kinetic energy by the specimen, was estimated for the present application as $28\times t_W$ which yields 2.5×10^{-4} s. This concept of transition time was validated by Nakamura, for SE(B) cracked specimens, as the limit for decreasing of significant dynamic effects and he proposed that the evaluation of fracture parameters using static formulation yields acceptable accuracy for time greater than $2\times t_T$. In the present application this transition

time is significantly greater than the stress wave reflection time in the Charpy specimen, thus neglecting the dilatational stress wave effects by static analysis is justifiable.

The analysis of the Charpy impact test using the finite element method requires a proper methodology which simulates failure initiation due to impact loading and crack propagation, by cleavage or ductile tearing, up to the final fracture of the specimen. In the present work the CBDD model was used in the calculation of the Charpy impact energy absorbed in breaking the specimen. The energy was computed by integrating the applied force versus load line displacement curve. This value included the work done in bending the specimen up to the point of fracture initiation and the work done in crack propagation. For the Charpy specimen geometry advantage was taken of double symmetry to model just one quarter of the geometry using the appropriate boundary conditions to represent the full specimen behaviour, with the finite element mesh shown in Fig. 10. This was derived after a sensitivity analysis of the mesh refinement to arrive at a sufficiently fine mesh.

The uniaxial strain rate-dependent material tensile properties and the critical stress, σ_u, were used as the input data, as described above. The critical stress, σ_u, values are summarized in Table 2 for the corresponding temperatures. The variations of the critical stress, σ_u, and m with temperature were the outcome of the tuning process using the experimental values of the fracture toughness for this material, available from Ref. [7], which were the best fit using the CBDD model for initiation of fracture for the cracked three point bend fracture toughness specimen, as discussed previously. The results of the Charpy impact energy are presented in Fig. 11 where the respective experimental results are also plotted for comparison. The maximum values for the local approach parameters at different temperatures are plotted in Figs. 7–9.

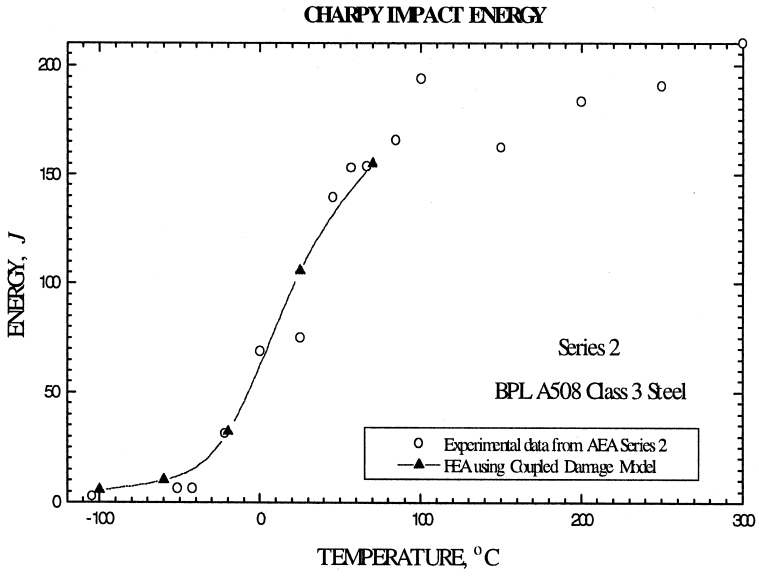

Fig. 11. Charpy impact energy for BPL A508 Series 2 material. The experimental data are from an AEA report [7] and the FEA results using the coupled brittle–ductileDamage model are ploted.

4.3. Correlation between fracture toughness and Charpy impact energy

The results of the FEA for both geometries in the transition temperature range were compared in an attempt to find some correlation between some of the local approach parameters. A summary of these results is plotted in Figs. 7–9 for either the Charpy geometry or the fracture toughness three-point bend specimen. The formulation of Wallin was used to predict the fracture toughness for prescribed values of probability of failure 5%, 50% and 95% from the transition temperature for which the Charpy energy is 28 J. These results are plotted in Fig. 6, where the results of the FEA using the coupled brittle–ductile damage model are also included. The numerical predictions for the Charpy energy are in good agreement with experimental data and the temperature for which the energy value is 28 J is −20°C. The Wallin formulation to obtain the fracture toughness from the Charpy transition temperature is

$$K_{IC} = 20 + \{11 + 77\exp(0.019[T - TK_{28J} + 18C + T_k])\}\left(\frac{25}{B_e}\right)^{1/4}\left(\ln\frac{1}{1-P_f}\right)^{1/4} \tag{8}$$

where TK_{28J} corresponds to the Charpy 28 J impact energy transition temperature, P_f is the desired failure probability, B_e is the effective length of the crack front, T is the usage temperature and T_κ describes the correlation scatter [5].

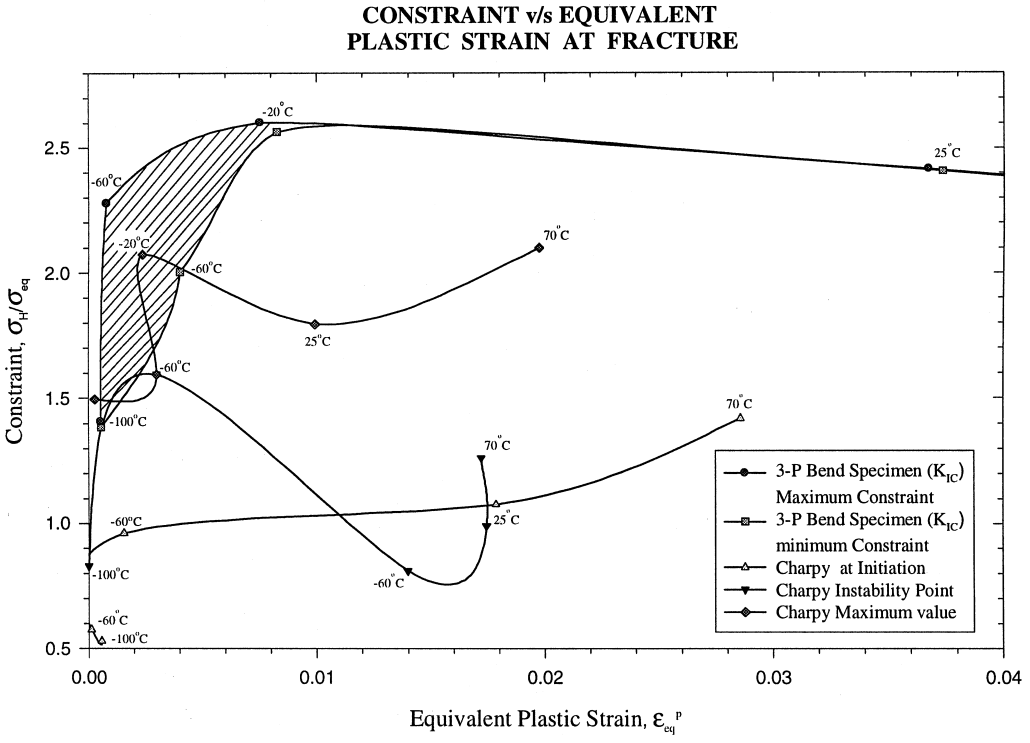

Fig. 12. FEA results of constraint and equivalent plastic strain that produced fracture in the three-point bend specimen and the Charpy specimen for the BPL A508 steel.

The constraint, σ_H/σ_{eq}, and the equivalent plastic strain, ε_{eq}, values which produced fracture in both geometries were calculated and analysed for all temperatures considered. The maximum values of constraint found for both specimens are compared in Fig. 12, which includes the corresponding equivalent plastic strain values. It should be emphasised that in Fig. 12 the values for the three-point bend specimen are the maximum and minimum for initiation of crack growth, whilst the values of the Charpy specimen are included for three conditions; at fracture initiation, at the instability point or final fracture and the highest at any point during the fracture process.

5. Discussion

The analysis of the Charpy specimen under impact loading by means of static analysis, simulating the change in material properties as a function of the strain rate, has proved to be successful. This way the vibration and noise produced by the stress waves in this small specimen are effectively avoided without penalising the accuracy of the results, as can be seen in the values of fracture energy presented in Fig. 10. It should be emphasised that the strain rate experienced at the root of notch in the Charpy specimen is much higher than that found in tensile specimens due to the combined effect of the notch, impact bend loading, lateral expansion and square transversal section. A notch increases the yield stress by strain rate and strain hardening effects and the effective stress below the notch is also raised by plastic constraint below the notch [22]. The material dependency on the strain rate in the Charpy specimen is much more severe than in an ordinary tensile test, thus it produces an increase of the yield stress which is very significant and which has an important effect on the mechanical properties of the materials. The conditions for initiation and propagation of a crack in the notched Charpy geometry were fully covered by using the modified Beremin and Lemaitre models as the local fracture criteria. Thus the crack advance was monitored in several steps allowing the measurement of the local approach parameters during the whole fracture process.

The onset of total brittle crack propagation of the Charpy specimen was determined by the lack of convergence of the program when the elastic modulus of the failed elements was sharply reduced. Final fracture in the transition and upper shelf zones, on the other hand, was again produced by lack of convergence but this time excessive strain was the cause. The crack advance for these temperatures in the Charpy specimen did not necessarily spread across the entire ligament but it is commonly observed experimentally in the ductile tearing range that the specimen does not fracture completely but tears and bends sufficiently to pass through the anvils of the testing machine.

The predictions of Charpy impact energy by means of the coupled brittle–ductile damage model are in good agreement with experimental data. The values of the parameters in the model responsible for the fracture criteria are critical in its response and the calibration of these by the trial and error procedure described above requires the previous knowledge of experimental values of cleavage stress, or fracture toughness or fracture values for notched tensile test. Good prediction of fracture initiation and crack propagation can be achieved with this numerical method at a low cost and many internal local approach parameters can be calculated at any point of the fracture process. The ductile crack growth initiation in the three-

point bend specimen at the temperature 70°C allowed the critical value for the damage variable to be determined which predicted the shear lips for the temperatures in the upper shelf of the Charpy energy transition curve. Likewise the critical cleavage stress, σ_u, and the Weibull distribution shape parameter, m, were determined from the previous knowledge of the fracture toughness at the subzero temperatures. The determination of the Charpy energy transition curve using the present model allows the temperature at which the energy is 28 J to be effectively calculated for application of the Wallin correlation.

The calibration of the numerical results for the three-point bend specimen with the experimental data has given impressive agreement of the change of failure mode with temperature as recorded in the AEA experimental data [7]. The additional analyses with the probability of failure set at 5% and 95% provided the lower and upper limits for the scatter in the experimental results. These also reflected the observed change in the failure mode for the different temperatures. In Fig. 6 the initiation of crack growth indicated by the reference data [7] was by brittle fracture for the temperatures −100, −60, −20 and 25°C for the probability of failure 0.05 (5%) and 0.5 (50%), but the initiation of crack growth was by ductile tearing for 70°C. On the other hand, for the probability of failure 95% just the specimens tested at subzero temperatures (−100, −60 and −20°C) failed by cleavage, while for the temperatures 25 and 70°C the initiation of crack growth was by ductile tearing. Therefore, the limit predicted for the brittle initiation of crack growth, for the bend specimen, is 300 MPa $m^{1/2}$, which is very close to the value 290 MPa $m^{1/2}$, determined experimentally, reported by Ortner et al. [7].

The coupled brittle–ductile damage (CBDD) model developed in the present work uses the same mesh size for both brittle and ductile failure, thus a mesh independence was introduced. The model uses a mesh size larger than the ideal recommended for the application of the Beremin model, namely 50 μm. This is an advantage, particularly for three-dimensional applications where the number of elements increases in geometrical proportion the computer memory and CPU time requirements. This special feature of the CBDD model relies upon the calculation of the failure probability for every element in the geometry instead of applying the Beremin model as a function of the Weibull stress for the whole geometry. Therefore, this probability of failure depends on the value of the maximum principal stress within an individual element, which should be almost constant. This application of the Beremin model requires that the mesh size should be such that the stress gradient in the elements is very low. The example of the stress gradients in the few elements ahead of the crack tip, for different sizes of mesh, in Fig. 5 shows that the mesh size can be successfully increased for the 3D elements, whilst retaining reasonable agreement with the plane strain formulation for 2D elements. The 3D elements produced a curve for the maximum principal stress distribution ahead of the crack tip which approximates the results for the 2D elements, although the elements are larger and due account of the effect of transversal stress on the 3D results has been taken. Hence the probability of brittle fracture for one 3D element, according to the formulation presented in Section 3.1, is equivalent to the probability of a number of smaller 2D elements with equal stress and a total area equivalent to that of the 3D element. It should be emphasised that 3D FEA requires a large number of unnecessary elements along the thickness, where the stress gradient is not so pronounced, in order to match the volume recommended equivalent to 2D elements formulation [5,12,18].

The variability of the two parameter cleavage stress, σ_u, and shape parameter, m, in the Beremin model with temperature was a direct consequence of the calibration of the numeric model with the experimental data. A scatter in the experimental results of the effective tensile stress at pure cleavage fracture for subzero temperatures was reported by Ortner et al. [7]. Moreover, Wiesner [24] presented results for the application of the Beremin model, based on the Weibull stress for the whole geometry, where σ_u and m varied considerably with temperature in the Charpy specimen geometry. The early experimental work of Ritchie et al. [25] predicted that the cleavage stress remains constant for a wide range of temperatures, for a mild high-nitrogen steel, but this value is determined when brittle fracture coincides with the yielding of the material. Other authors also considered σ_u and m as constants over a range of temperature [26, 27], in 2D plane strain FE analyses for the BPL A508 steel of a 80 mm SE(B) specimen. In the present application the parameter σ_u in the Beremin model is believed to be a scale parameter, which is linked to the actual cleavage stress of the material, but may vary somewhat with temperature. This may be the case because the probability of ductile fracture increases with temperature and the experimental data for the lower temperatures force the value of the σ_u down. The results of the present work suggest that the cleavage stress would be between 1875 and 2100 MPa, if the Charpy transition temperature TK_{28J} and the fracture toughness limit of 300 MPa $m^{1/2}$ for the onset of upper shelf are considered, respectively, as an equivalent to Ritchie et al.'s definition of cleavage stress [24].

The application of the Wallin correlation produced very good predictions for fracture toughness. This shows that the correlation between the temperature for which the Charpy energy is 28 J and the temperature for which the fracture toughness is equal to 100 MPa $m^{1/2}$ is very consistent. The transition temperature in the Charpy energy, TK_{27J}, is $-20°C$ and the temperatures at which the fracture toughness is 100 MPa $m^{1/2}$ are $-36°C$ for the experimental data and $-32°C$ for the numerical results. The ΔT for the experimental data and the numerical data are 16 and 12°C, respectively, which are consistent with the 18°C mean temperature difference reported by Wallin [5].

From Fig. 7 it can be seen that the constraint, σ_H/σ_{eq}, and maximum principal stress/cleavage stress ratio, σ_1/σ_u, for both specimens are of the same order of magnitude. However, the axial or longitudinal stress/yield stress ratio, σ_{11}/σ_y, can be double the values of the above parameters. It is interesting to notice that the maximum σ_{11}/σ_y ratios for both specimens present the same pattern, that is, increasing with temperature but falling for ductile fracture at the temperature 70°C. On the other hand the constraint shows a different pattern for the three-point bend specimen and for the Charpy specimen as can be seen in Fig. 8. The semi-elliptical shape of the constraint curve for the three-point bend specimen is very distinctive and both specimens present the peak values at $-20°C$. The maximum principal stress/cleavage stress ratios, σ_1/σ_u, included in Fig. 9 show an intersection for temperatures -16 and 50°C for the Charpy specimen at final fracture and the three-point bend specimen at initiation.

The results of the numerical analyses using the coupled brittle–ductile damage model, shown in Fig. 6, suggest that the Wallin formulation appears slightly over conservative for the higher temperatures where ductile damage took place. This could be due to the brittle fracture basis of the Wallin correlation, which very accurately predicted the fracture toughness for values under 600 MPa $m^{1/2}$. The Wallin formulation seems to follow the brittle fracture pattern right up to very high temperatures at which ductile tearing produces initiation of crack growth for

stress levels below the required for cleavage. The surprisingly simple to use Wallin equation produces excellent estimates for the nuclear industry steel with the only requirement being the transition temperature for Charpy energy 28 J, which is simple to obtain experimentally.

The results of the combination of constraint, hydrostatic stress/equivalent stress ratio and equivalent plastic strain that produce failure for the three-point bend specimen in Fig. 12, show that the gap between maximum and minimum constraint closes for temperatures above -20°C. The shaded area in Fig. 12 shows the area of combination of constraint-equivalent plastic strain, which produces failure for the three-point bend specimen right before the peak of the values. The maximum value of constraint and the corresponding equivalent plastic strain obtained for the Charpy specimen at the temperature -20°C are the only values inside the critical shaded area of the fracture toughness results. This is the most likely explanation for the correlation between the temperatures for Charpy energy value 28 J and fracture toughness value of 100 MPa $m^{1/2}$. The values of constraint-equivalent plastic strain that produced initiation of fracture in the Charpy specimen and the final fracture are considerably lower than those for the fracture toughness specimen. The values for final fracture in the Charpy specimen for the lower temperatures are closer to the critical area of possible combinations in the fracture toughness specimen. The crack extension for the Charpy specimen at -20°C at the point of the maximum value of constraint is 3.5 mm at mid-thickness, a/W equal to 0.4375, very close to the crack extension of the three-point bend specimen. Furthermore, the fracture mechanism in the Charpy specimen, at this particular temperature, is pure brittle fracture producing a controlled crack growth up to the point of the peak of constraint after which the crack became unstable.

6. Conclusion

The coupled brittle–ductile damage model based on a combination of modified Beremin and Lemaitre models has been used to analyse the behaviour of a standard fracture toughness bend test and the Charpy V notch impact test. Local approach 3D finite element analyses for state of stress and strain were used to determine critical values of fracture stress or plastic strain and constraint in the two specimen geometries. The critical values were calibrated from experimental data for fracture toughness on an A508 Class 3 steel and these same values were then used to predict the Charpy impact test transition curve after modifying the material stress strain properties to allow for strain rate effects in the Charpy test. For the fracture toughness specimens, the calibration to fit numerical values also led to excellent predictions in the model as to whether fracture occurred by brittle or ductile modes. The agreement between the experimental data and the predicted Charpy transition curve was also excellent.

The correlation proposed by Wallin between temperature for fracture toughness at 100 MPa $m^{1/2}$ and the Charpy transition temperature TK_{28J} was well demonstrated by the experimental data and by the predictions of the CBDD model. Particularly for the brittle regime the Wallin formulation produced very accurate results and prescribed failure probability of 5% and 95% provide a good interval of confidence for the scatter of experimental data.

The results of the numerical analyses have shown a possible explanation for the correlation between temperatures for about 27 or 28 J Charpy energy absorption in the Charpy test and

fracture toughness values of 100 MPa $m^{1/2}$. The values of the local approach parameters obtained with the CBDD model applied to the A508 steel suggest that the level of triaxial stress state and the plastic strain of the material are very similar at the particular temperature where the Charpy specimen energy absorption is 27 J and the fracture toughness is 100 MPa $m^{1/2}$. The results seem to provide strong evidence that the triaxial stress state and plastic strain in the material reach a critical level, despite the differences in geometry, strain rate, notch acuity and specimen size. This result suggests that the local approach parameters, σ_H/σ_{eq} and ε_{eq} are independent of geometry effects and strain rate to characterize fracture, which is encouraging for transferability of small scale test results to large scale structures.

The number of parameters to be calibrated in the CBDD model is not large and the difficulties are not great to carry out the calibration when compared to the results which may be achieved. The coupled model is a powerful practical engineering tool.

Acknowledgements

The experimental data used in the present work were provided by AEA Technology and these are gratefully acknowledged.

References

[1] Hodgson J, Boyd GM. Brittle fracture in welded ships. Inst Naval Archit 1958;100(3):141–80.
[2] Shank ME. A critical survey of brittle failure in carbon plate steel structures other than ships. Welding Research Council Bulletin, No. 17, 1954.
[3] Barsom JM, Rolfe ST. Correlation between K_{IC} and Charpy V-notch test results in the transition-temperature range. In: Impact Testing of Metals, ASTM STP 466. American Society for Testing and Materials, Philadelphia, PA: , 1970. p. 281–302.
[4] Marandet B, Sanz G. Etude par la mecanique de la rupture de la tenacite d'aciers a resistance moyenne fournis en forte epaisseur. Rev Metall 1976;359–383.
[5] Wallin K. New improved methodology for selecting Charpy toughness criteria for thin high strength steels. Report presented to Commission X, IIW 1994 Annual Assembly, Beijing, IIW DOC. NO. X-1290-94, 1994.
[6] Phaal R, MacDonald KA, Brown PA. Correlation between fracture toughness and Charpy impact energy. TWI Report, The Weld Institute, December 1994.
[7] Ortner SR, Gibson GP, Wall M, Lane CE, Capel M, Druce SG. Heat treatment effects on the fracture toughness transition properties of the BPL A508 Class 3 steel forging. AEA Technology, AEA-TRS-4071, AEA Thermal Reactor Services, January 1991.
[8] ABAQUS standard user's manuals, version 5.5. Hibbit, Karlsson and Sorenson Inc, 1995.
[9] Beremin FM. A local criterion for cleavage fracture of a nuclear pressure vessel steel. Metall Trans A 1983;14:2277.
[10] Lemaitre J. A continuous damage mechanics model for ductile fracture. J Eng Mater Technol 1985;107:83.
[11] Folch LCA. Application of the local damage mechanics approach to transition temperature behaviour in steels. PhD. Thesis, University of Manchester Institute of Science and Technology, UMIST, Manchester, 1997.
[12] Gurson AL. Continuum theory of ductile rupture by void nucleation and growth. Part I—yield criteria and flow rules for porous ductile media. J Eng Mater Technol Trans ASME, 1977;.
[13] Ainsworth RA, O'Dowd NP. A framework for including constraint effects in the failure assessment diagram approach for fracture assessment. Report for TAGSI, TAGSI/FSG(94)P62, 1994.

[14] Hadley I. The use of the elastic T-stress and other constraint parameters in fracture mechanics. TWI Report, The Weld Institute. Abington, Cambridge: Abington Publishing, 1995.
[15] Hancock JW, Karstensen AD, MacLennan IJ, Nekkal A. Constraint estimation. Advances in Fracture Mechanics, TAGSI Symposium, Abington, Cambridge, January 1996.
[16] O'Dowd NP, Shih CF. Family of crack-tip fields characterized by a triaxiality parameter—II. fracture applications. J Mech Phys Solids 1992;40(5):939–63.
[17] Sherry AH, France CC, Goldthorpe MR. Compendium of T-stress solutions for two and three dimensional cracked geometries. Fract Engng Mater Struct 1995;18(1):141–55.
[18] Campbell JD. The yield of mild steel under impact loading. J Mech Phys Solids 1954;3(1):54–62.
[19] Gerard G, Papirno R, Becker H. On experimental solid dynamics. In: Symposium on Dynamic Behaviour of Materials, ASTM STP 336, 1962. p. 82–103.
[20] Bodner SR, Symond PS. Experimental and theoretical investigation of the plastic deformation of cantilever beams subjected to impulsive loading. Trans ASME J App Mech, 1962;.
[21] Nakamura T. Effects of rate-sensitivity in dynamically loaded 3D fracture specimen. In: Proceedings of the 7th International Conference on Fracture, Houston, TX, vol. 1, 1989. p. 795–802.
[22] Vargas PM, Dodds RH. Inelastic response of a deep crack single-edge notch specimen under impact loading. Work related to author's Ph.D. Thesis, University of Illinois, Urbana, IL, 1993.
[23] ASTM Standard E 813-89. Standard test method for I J_{IC}, a measure of fracture toughness. American Society for Testing and Materials, Philadelphia, PA.
[24] Wiesner CS. Investigation into temperature and specimen geometry dependence of the 'local approach' parameters of a structural steel. TWI Report, The Welding Institute, UK. August 1995.
[25] Ritchie RO, Knott JF, Rice JR. On the relationship between critical tensile stress and fracture toughness in mild steel. J Mech Phys Solids 1973;21:395–410.
[26] Goldthorpe R, Andrews RM, Wiesner CS. Fracture toughness predictions for a range of geometries using a coupled cleavage/ductile micromechanical model. In: Engineering Structural Integrity Assessment. Abington, Cambridge: TWI, Abington Publishing, 1996.
[27] Lidbury D, Sherry A et al. Application of the local approach to predict cleavage and ductile fracture. Advances in fracture mechanics, TAGSY Symposium, Abington, Cambridge, 1996.